

# **Rapid patterning and zonal differentiation in a two-dimensional *Dictyostelium* cell mass: the role of pH and ammonia**

S. Sawai, T. Hirano, Y. Maeda and Y. Sawada

10.1242/jeb.004408

There was an error published in *J. Exp. Biol.* **205**, 2583-2590.

The reference Hara and Konijn (1976) was incorrectly listed in the References. The name of the first author was inadvertently omitted and the reference should have been listed as:

**Nanjundiah, V., Hara, K. and Konijn, T. M.** (1976). Effect of temperature on morphogenetic oscillations of *Dictyostelium discoideum*. *Nature* **260**, 705.

The reference was also incorrectly cited in the first paragraph of the Discussion (p. 2586). The citation to (Hara and Konijn, 1976) should in fact have read (Nanjundiah et al., 1976).

We apologise to Dr Nanjundiah for this error.

## Rapid patterning and zonal differentiation in a two-dimensional *Dictyostelium* cell mass: the role of pH and ammonia

Satoshi Sawai<sup>1,\*</sup>, Takashi Hirano<sup>2</sup>, Yasuo Maeda<sup>2</sup> and Yasuji Sawada<sup>3</sup>

<sup>1</sup>Graduate School of Information Sciences, <sup>2</sup>Biological Institute, Graduate School of Science and <sup>3</sup>Research Institute of Electrical Communication, Tohoku University, 2-1-1 Katahira, Aoba-ku, Sendai 980-8577, Japan

\*Author for correspondence at present address: Princeton University, Department of Molecular Biology, Princeton, NJ 08544, USA  
(e-mail: ssawai@molbio.princeton.edu)

Accepted 20 May 2002

### Summary

Recently it was demonstrated that a rapidly forming, self-organizing pattern that emerges within two-dimensional *Dictyostelium discoideum* cell cultures could later give rise to stripes of distinct zones, each comprising different cell types. Here we report physiological aspects of the initial rapid patterning and its relationship to cell differentiation. We found that as the temperature is lowered the characteristic length of the pattern increases. From this we estimated the activation energy of the patterning kinetics. Fluorescence of fluorescein-conjugated dextran revealed that the cytosolic pH of cells in the inside zone becomes lower than that in the outer zone facing the air. The patterning could be inhibited by addition of the plasma-membrane proton pump inhibitors

diethylstilbestrol (DES) or miconazole. Preincubation of cells with weak acid delayed the timing of the patterning, whereas weak base hastened it. A pH-indicating dye revealed localized accumulation of ammonia in the extracellular space. These results suggest that gradients of secreted metabolites may be directly responsible for the rapid patterning and its consequence on cell differentiation in a confined geometrical situation. Possible diffusible candidate molecules and a reaction scheme coupled to the imposed oxygen gradient are discussed.

Key words: oxygen, pH, ammonia, H<sup>+</sup>-ATPase, reaction-diffusion, *Dictyostelium discoideum*.

### Introduction

In 1995, Bonner and his colleagues (Bonner et al., 1995) reported a rapid patterning phenomenon in *Dictyostelium* cells confined to a microcapillary tube. Within a few minutes of being trapped in such a confined geometrical space, cells show a strikingly vivid zonal pattern. Cells facing the air become motile and dark, whereas cells closer to the mineral oil seal at the other end of the capillary tube become round, less motile and brighter. When well-synchronized, early mound-stage cells are subjected to rapid patterning in two dimensions (2-D), early cell-type differentiation becomes position-dependent; *DI9*, *ecmB* and *ecmA* gene expression each appear as a band of distinct zones from the outermost domain of the outer zone to the border region between the inner and outer zones (Hirano et al., 2000).

Several lines of evidence suggest that the initial rapid patterning itself is not merely due to a threshold response to oxygen, but to a reaction-diffusion mechanism independent of the well-studied cAMP relaying system (Sawada et al., 1998; Bonner et al., 1998). The patterning has some required properties for Turing instability, which so far has only been realized in physico-chemical systems (Sawai et al., 2000). If so, what are the diffusive molecules involved and why do they evoke rapid cell shape change? Apart from interest in

the 'generic' patterning mechanism (Newman and Comper, 1990), our recent findings that prestalk cells initially appear in an outer region and prestalk cells in an inner region (Hirano et al., 2000) were contradictory to the earlier prediction of Bonner and colleagues (Bonner et al., 1998). According to their theory (Bonner et al., 1998), the main environmental factor which gives preference to the cell-type fate is oxygen (Sternfeld, 1988); thus one would expect prestalk cells to appear in the outer region facing the air. If not oxygen, what biases the fate of the cells in the confined 2-D culture?

In this report, we sought to answer the above questions by looking at the physiological aspects of the initial patterning. Temperature dependence was studied to determine the activation energy of the kinetics as well as its effect on zonal differentiation. We then show that rapid alteration in the cytosolic pH (pHi) and ammonia secretion take place during the patterning. The observed zonal-differentiation pattern supports the proposed relationship between intracellular pH and cell-type differentiation of *Dictyostelium* cells based on monolayer and other *in vitro* assays. A possible reaction scheme of the rapid patterning and its relationship to cell differentiation in a confined culture is discussed.

## Materials and methods

### Cell growth and development

*Dictyostelium discoideum* strain Ax-2 cells were grown in PS medium (Hirano et al., 2000) and shaken in Erlenmeyer flasks at  $150 \text{ revs min}^{-1}$  at  $22^\circ\text{C}$ . Cells were collected before they reached a density of  $5 \times 10^6 \text{ cells ml}^{-1}$  and thus were in log phase. Wild-type NC-4 cells were grown with *E. coli* B/r on a nutrient agar plate (Bonner, 1947). To obtain a synchronized population of early mound-stage cells, we followed the method of Hirano et al. (2000). Growth-phase cells were washed twice with Bonner's salt solution (BSS; 0.6 g NaCl, 0.75 g KCl, 0.3 g  $\text{CaCl}_2$  in 1 l distilled deionized water; Bonner, 1947) and suspended at a density of  $5.0 \times 10^7 \text{ ml}^{-1}$ . 1 ml of the cell suspension was plated on 1.5% agar in a 90 mm plastic dish. The plate was incubated at  $22^\circ\text{C}$  for 2 h, followed by overnight incubation at  $4^\circ\text{C}$ . The plate was then shifted back to  $22^\circ\text{C}$  and allowed to develop for 3–3.5 h.

### 2-D culturing

A cell mass confined between two glass plates was prepared as previously described (Sawada et al., 1998). Cells were pelleted by centrifugation and the supernatant was removed. Cells were carefully collected from the tube with a Pasteur pipette and placed on a microscope slide. Two spacers of approximately  $100 \mu\text{m}$  thickness were placed beside the cell mass and the coverslip was immediately laid on top of the cell mass and the spacers; this time is denoted as  $t=0$ . The culture was kept on a plastic plate together with wet paper towels to maintain the humidity above 95%. Measurements were performed under an Olympus IMT-2 microscope equipped with a Sony CCD-IRIS camera. For some of the measurements, time-lapse recording and video capturing were employed. A CCD camera was connected to a Hi8 VISCA system controlled by a Macintosh computer running NIH Image software.

### Fluorescent labeling

For loading of fluorescein conjugated with dextran ( $M_r=1 \times 10^5$ ; Molecular Probes), cells were washed twice with PB ( $20 \text{ mmol l}^{-1}$  sodium/potassium phosphate buffer, pH 6.5) and suspended at a density of  $5.0 \times 10^7 \text{ cells ml}^{-1}$  in the same buffer containing  $1 \text{ mg ml}^{-1}$  of the dextran. Loading of the fluorescent probe was achieved by applying, at 5 s intervals, two exponentially decaying pulses of  $2 \text{ kV cm}^{-1}$  with a time constant of 0.7 ms using a simple circuit described by Yumura et al. (1995) at  $2.2 \mu\text{F}$  capacitance. Electroporated cells were immediately suspended in a healing solution (PB, pH 6.5, containing  $2 \text{ mmol l}^{-1}$   $\text{MgCl}_2$  and  $0.2 \text{ mmol l}^{-1}$   $\text{CaCl}_2$ ) (van Haastert et al., 1989) for 10–15 min on ice and washed twice with PB.

### Temperature control

Temperature dependence of the pattern size was measured by constructing a transparent vessel which let a thin layer of water (approximately 1 mm) run beneath a glass plate where the sample was kept. The temperature of the water was controlled by a circulator (Coolnics CTE-22W, Komatsu) from

$2\text{--}40^\circ\text{C}$ . The temperature of the sample was read by a thin metal sensor placed on the sample plate. Conical tubes containing pelleted cells were placed on ice and used

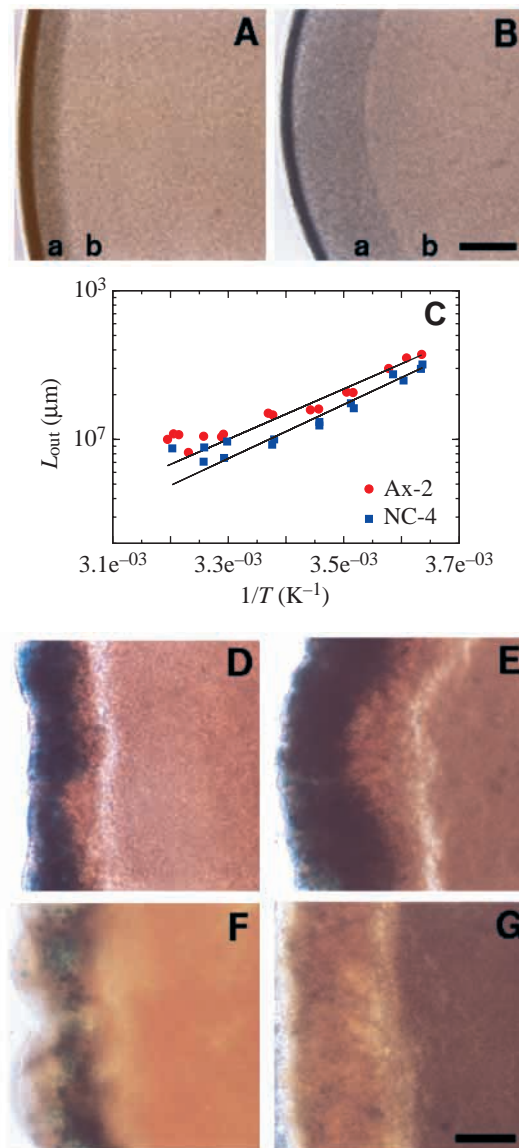


Fig. 1. (A,B) Dependence of the outer zone depth on temperature in 2-D cultures. a, outer zone; b, inner zone. The dark outermost edge is a meniscus. Freshly starved NC-4 cells at (A)  $30^\circ\text{C}$ , 10 min after preparation, and (B)  $4.5^\circ\text{C}$ , 15 min after preparation. (C) Freshly starved NC-4 and Ax-2 cells were two-dimensionally cultured in an isothermal vessel. Each plot represents a 1–2 h time average of the outer zone depth  $L_{\text{out}}$ . Plots are fitted by  $L_{\text{out}} \propto \sqrt{T \exp(E/2RT)}$ , where  $T$  is absolute temperature (K) and  $R$  is the gas constant, giving activation energy of  $E=65 \text{ kJ mol}^{-1}$ ,  $E=69 \text{ kJ mol}^{-1}$  for Ax-2 and NC-4 cells, respectively. Plots at  $40^\circ\text{C}$  have been omitted for the curve fitting. (D–G) Temperature dependence on cell differentiation. Early-mound stage cells were subjected to 2-D culture. Cells at the outermost region of the outer zone show *D19* expression at both  $22^\circ\text{C}$ ,  $t=4$  h (D) and  $10^\circ\text{C}$ ,  $t=4$  h (E). The *ecmB* expression observed near the border at  $22^\circ\text{C}$  ( $t=2$  h) (F) is suppressed at  $10^\circ\text{C}$  ( $t=3$  h) (G). Scale bars,  $200 \mu\text{m}$  (A,B);  $100 \mu\text{m}$  (C,D).

immediately to prepare a sample in the vessel. Fixation and X-gal staining of transformed cells bearing the reporter *lacZ* gene under the control of cell type-specific promoters were performed as described previously (Hirano et al., 2000).

#### Proton pump inhibition, weak acid and base loading

Following the method described by Inouye (1988), washed cells were suspended for 5–10 min either in PB (pH 6.0) or BSS containing 20  $\mu$ mol diethylstilbestrol (DES) or miconazole. For weak acid treatment, cells were suspended in PB (pH 6.0) containing 20 mmol propionic acid sodium salt or 5,5-dimethyl-2,4-oxazolidinedione (DMO). Similarly 0–20 mmol<sup>-1</sup> NH<sub>4</sub>Cl or methylamine was added to PB (pH 8.0). Cells were immediately pelleted by centrifugation without washing and used in the 2-D culture chamber to observe patterning. DES, miconazole, propionate, DMO, and methylamine were purchased from Sigma.

#### Detection of extracellular pH

Bromocresol Purple was added to the cell suspension (0.02–0.04 % in BSS) just before preparing the pellet for a 2-D culture. For detection of ammonia, a drop of the cell-free Bromocresol Purple solution was placed approximately 1 cm away from the cell mass to detect any change in the external pH (pHe).

## Results

#### Effect of temperature on pattern size and cell differentiation

A rapid pattern emerged at all the temperatures we tested, ranging from 2 to 40 °C. As shown in Fig. 1A,B, the length of the outer zone increases as temperature is lowered. Fig. 1C shows the plot of outer zone depth  $L_{out}$  against the inverse of absolute temperature  $T$ . It is clear that  $L \propto \exp(1/T)$ , which is

consistent with other evidence that the patterning is due to a reaction-diffusion mechanism (see Discussion) (Bonner et al., 1998; Sawai et al., 2000).

The effect of low temperature on zonal differentiation was also studied. Fig. 1D–G shows the expression pattern of the prespore-specific *D19* and prestalk-specific *ecmB* genes observed under our experimental conditions at 22 °C and 10 °C. A region where *D19* gene expression is first observed always appears at the outermost domain and is relatively longer in width when the outer zone is expanded at the low temperature. In contrast, *ecmB* expression is almost completely suppressed at 10 °C.

#### pH effects

Relative change in pHi was observed using fluorescein, whose fluorescence decreases as the pH is lowered (Haugland, 1996). As shown in Fig. 2, the pHi of cells in the inner zone is relatively lower than that of the outer zone cells, with a sharp transition at their border. The time required for such a pHi gradient to become established is almost the same as that of the appearance of the dark and bright patterns observed by transmitted light. From the difference in the fluorescence intensity, if one assumes the highest value of pHi to be around 7.5, there could be a difference of more than 0.5 pH units between the two zones.

We detected changes in the extracellular pH by adding Bromocresol Purple (pH 5.2, yellow; pH 6.8, purple) to the suspension just before preparing a pellet. As shown in Fig. 3A, we observed alkalinization of the extracellular medium in the outer zone, whereas that of the inner zone remained acidic. The change in color occurred simultaneously with the rapid emergence of the pattern itself. When a drop of the same Bromocresol Purple solution was placed separately from the sample, we could also see the same change in color from

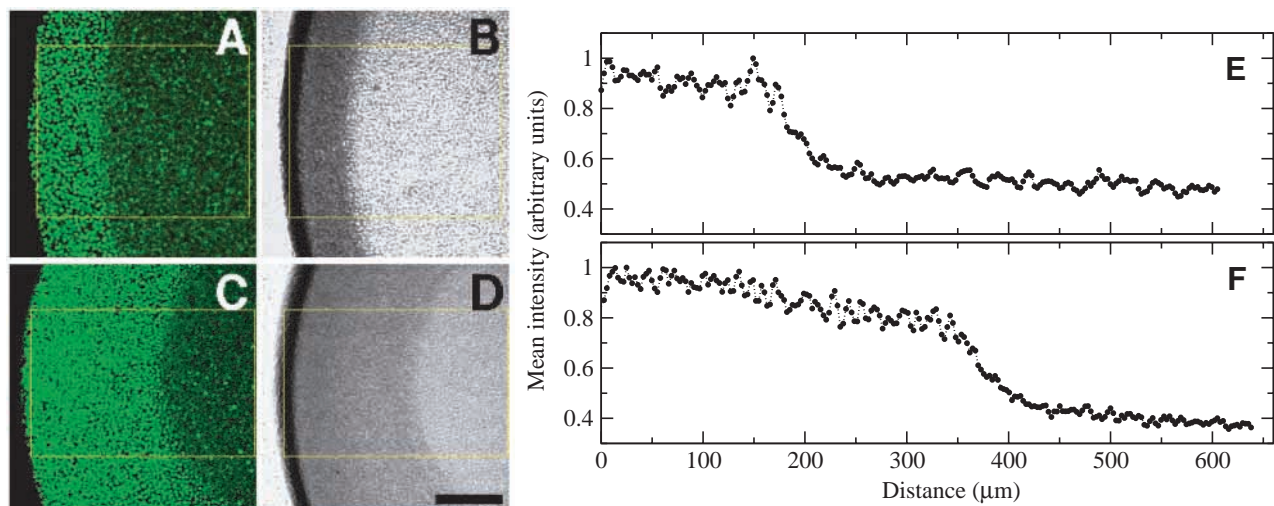


Fig. 2. Cytosolic pH change and patterning. (A,B) Cells were grown in atmospheric oxygen or (C,D) 100 % O<sub>2</sub>. (A,C) Fluorescence intensity obtained by confocal microscopy; excitation at 488 nm and 510–550 nm band pass filter. (B,D) Transmitted light. (E,F) Fluorescence intensity averaged over the vertical direction in the indicated boxes. Low fluorescence intensity in the inner-zone cells suggests acidification of their cytosolic pH.

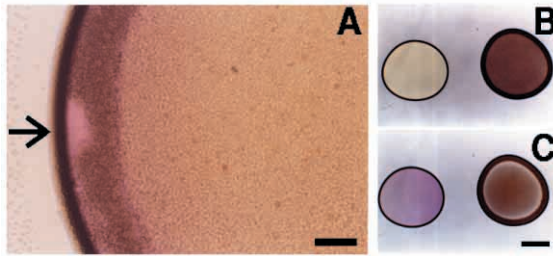


Fig. 3. Extracellular pH change demonstrated by Bromocresol Purple (pH 5.2, yellow; pH 6.8, purple). (A) Alkalinization of extracellular space in the outer zone,  $t=1$  h, 7 min. The arrow shows a position partially deprived of cells to show the change in color more clearly. (B,C) A drop of Bromocresol Purple solution (left) kept at a distance from a 2-D cell mass (right) also changes color after (B)  $t=15$  min and (C)  $t=2$  h, 44 min. Scale bars,  $100\text{ }\mu\text{m}$  (A);  $1\text{ mm}$  (B,C).

yellow to purple (Fig. 3B). This indicates that at least one of the diffusive molecules responsible for the rise in extracellular pH is volatile, and was possibly ammonia. We did not observe the staining pattern when cells were incubated for 10 min with Bromocresol Purple and then washed before preparing the 2-D culture. Intake of the dye is minimized under our experimental conditions, and the color mainly represents the pH of the extracellular space. The arrow in Fig. 3A shows that the change in color is observed where there are no cells.

#### *Effect of weak acid, proton pump inhibitors and weak base*

Fig. 4 shows the effect of proton pump inhibitors. When cells were pre-incubated with either  $10\text{ }\mu\text{mol l}^{-1}$  DES or  $10\text{ }\mu\text{mol l}^{-1}$  miconazole, the patterning became almost undetectable. The effect was almost negligible with inhibitors at  $5\text{ }\mu\text{mol l}^{-1}$ , and the distinction between the two zones was the same as in the controls. Preincubation at concentrations above  $10\text{ }\mu\text{mol l}^{-1}$  ( $\leq 50\text{ }\mu\text{mol l}^{-1}$ ) had a stronger pattern-erasing effect. 0.5% ethanol, used as a solvent, had no effect on the rapid patterning when added alone. The effective concentrations of these inhibitors are close to those reported to inhibit the plasma membrane proton pump in *Dictyostelium* cells and to lower the pHi (Inouye, 1989; van Duijn and Vogelzang, 1989).

When freshly starved cells were preincubated with  $10\text{--}20\text{ mmol l}^{-1}$  sodium propionate at pHe 6.0 before sample preparation, there was a concentration-dependent delay in the onset of the patterning (Fig. 5A). When the same experiment was conducted at pHe 8.0, there was no noticeable effect on the patterning, indicating that the active molecule is the neutral form of propionate, which is more membrane permeable than its ionized form. The same effect was observed when DMO was used instead of propionate (Fig. 5C).

When freshly starved cells were pre-incubated with  $5\text{--}20\text{ mmol l}^{-1}$  ammonia at pHe 8.0, patterning occurred very rapidly, and was almost complete within 1 min (Fig. 5B). The same treatment at pHe 6.0 had no effect, indicating again that  $\text{NH}_3$  rather than  $\text{NH}_4^+$  is the active species. The same effect was observed when methylamine was used instead of ammonia (Fig. 5C).

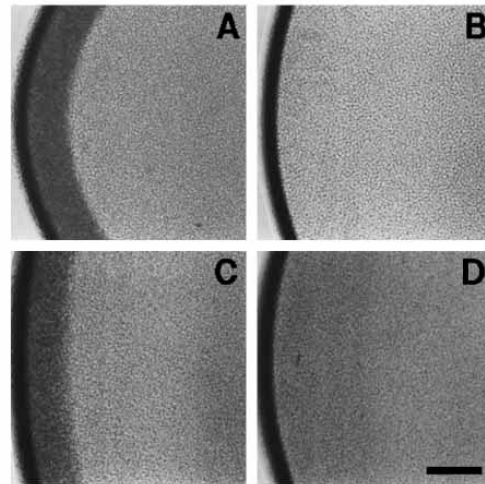


Fig. 4. Effect of proton pump inhibitors. Ax-2 cells were pre-incubated with (A)  $5\text{ }\mu\text{mol l}^{-1}$  or (B)  $10\text{ }\mu\text{mol l}^{-1}$  DES, and (C)  $5\text{ }\mu\text{mol l}^{-1}$  or (D)  $10\text{ }\mu\text{mol l}^{-1}$  miconazole, prior to 2-D culturing. Photographs were taken at  $t=30$  min (A,B) and  $t=10$  min (C,D). Scale bar,  $200\text{ }\mu\text{m}$ .

## Discussion

### *Temperature*

Similar temperature dependence of patterning was first reported by Harrison et al. (1981) in whorls of *Acetabularia mediterranea*. If a spatial pattern were to emerge from reaction and diffusion, dimensional analysis tells us that the length should be proportional to the geometric mean of the diffusion coefficient  $D$  divided by the kinetic rate constant  $k$ . If we suppose that  $D$  follows the Einstein relation  $D \propto T$ , and the Arrhenius law  $k \propto \exp(-E/RT)$ , where  $E$  is activation energy and  $R$  the gas constant, it follows that  $L_{\text{out}} \propto \sqrt{T \exp(E/2RT)}$ . From Fig. 2C,  $E=65\text{ kJ mol}^{-1}$  for Ax-2 cells and  $E=69\text{ kJ mol}^{-1}$  for NC-4 cells. These values may be interpreted as the activation energy of a rate-limiting step in the entire reaction scheme discussed below. A similar value of  $E$  (approx.  $67\text{ kJ mol}^{-1}$ ) was reported for cAMP oscillations of *Dictyostelium* (Wurster, 1976), and both are values in the range of activation energies for non-transport enzyme-catalysed reactions (Hara and Konijn, 1976).

While *D19* expression remained constant, strong *ecmB* expression characteristic of 2-D culturing was suppressed at low temperatures. These results are similar to the changes observed under high  $\text{O}_2$  environments (Hirano et al., 2000). It should be noted that in both high oxygen and low temperature, depth of the weak-base-rich outer zone is increased. This change in *ecmB* expression is consistent with the idea that a decrease in ammonia plays a part in switching from the slug stage to the fruiting body formation (Singleton et al., 1998).

### *Cytosolic pH*

We present evidence that rapid patterning is closely linked to changes in pHi in *Dictyostelium*. It is well known that the pHi of *Dictyostelium* cells is lowered by incubation with weak

acid such as propionate and DMO, or by plasma membrane proton pump inhibitors such as DES and miconazole (Inouye, 1989; van Duijn and Vogelzang, 1989). In our present study, cells in the outer zone, which are darker and more motile than those in the inner zone, have a relatively high pHi. DES and miconazole at low concentrations known to inhibit plasma membrane proton pump cause the pattern to disappear, suggesting that pHi regulation is an essential part of the patterning response. A previous report of pattern inhibition by azide (Hirano et al., 2000) could also be explained not by energy depletion but by inhibition of the plasma membrane proton pump activity, as reported by van Duijn and his colleagues (van Duijn et al., 1990). Change in timing of the patterning by weak acid and weak base should be caused by an alteration of the initial pHi and also in the buffering capacity of the cells.

The observed pHi gradient is similar to that reported by Azhar and Nanjundiah (1996) using fluorescence of Neutral Red, except that they found that acidification was more localized around the border between the two zones. The reason for this difference could be due both to the fact that Neutral Red reflects the pH of acidic compartments rather than the cytosol, and also that there is a difference in the oxygen gradient present in their 1-D experimental design, which permits a secondary peak of weak base to appear in the inner region.

The fact that motile cells in the outer zone have higher pHi is consistent with our current knowledge of pHi and cell motility of *Dictyostelium* cells (van Duijn and Inouye, 1991). In contrast, cells in the inner zone have a lower pHi and are less motile. An actin-binding protein, hisactophilin, is known to bind along actin filaments only when the pH is <7.2 (Stoekelhuber et al., 1996). Thus the difference in levels of transmitted light between the inner and outer zones could reflect an alteration in cortical actin assemblies. It would still be an oversimplification, however, to attribute cell-shape differences only to a pH change. Other effects, such as tyrosine phosphorylation of actin, are also known to occur under conditions of low oxygen or DNP treatment (Jungbluth et al., 1994) and should be carefully taken into account in future studies.

It may also be possible that patterning is more directly related to the plasma membrane potential than to pH or other ions, since the DES- and miconazole-sensitive plasma membrane H<sup>+</sup>-ATPase (Pogge-von Strandmann et al., 1984) is the major generator of the membrane potential in *Dictyostelium* (van Duijn and Vogelzang, 1989). However, TMRM (tetramethyl rhodamine methyl ester), a dye that distributes

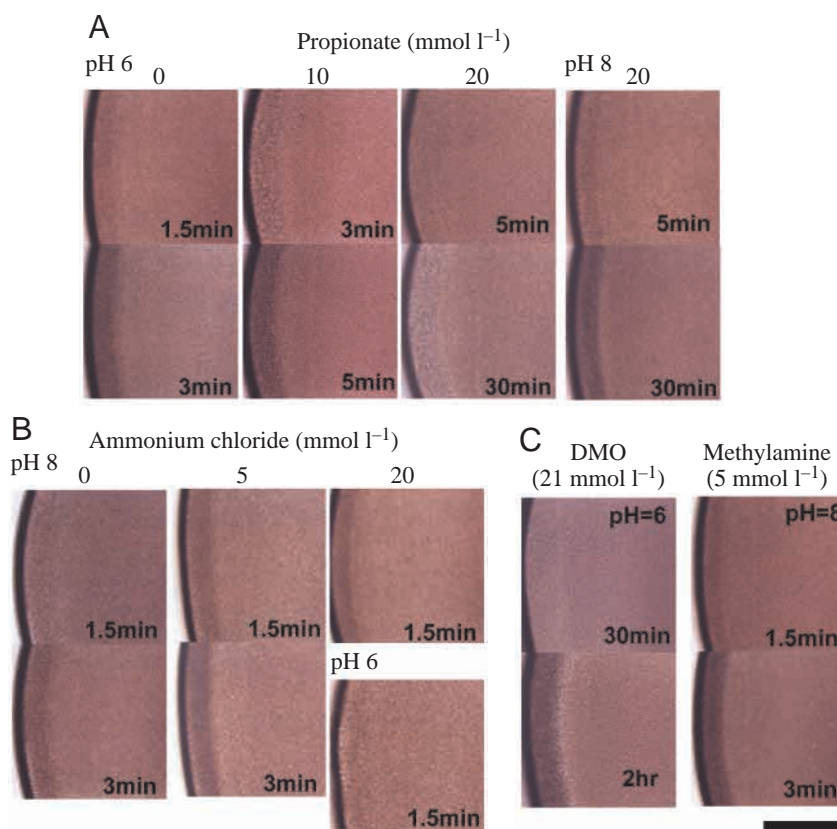


Fig. 5. Freshly starved Ax-2 cells pre-incubated for 15 min in weak acid or weak base show an altered timing of rapid patterning. (A) 0–20 mmol l<sup>-1</sup> sodium propionate added to PB delays the patterning in a concentration-dependent manner at pH 6, but no effect was seen at pH 8. (B) The pattern becomes visible at  $t=1.5$  min when cells are preincubated in 5 mmol l<sup>-1</sup> NH<sub>4</sub>Cl at pH 8, whereas in the control it only becomes visible at  $t=3$ –5 min. The same effect is seen in 20 mmol l<sup>-1</sup> NH<sub>4</sub>Cl at pH 8 but not at pH 6. (C) Similarly, the weak acid 5,5-dimethyl-2,4-oxazolidinedione (DMO) delays the patterning, and the weak base methylamine hastens it. Scale bar, 400  $\mu$ m.

across the cell membrane according to the Nerntian potential (Ehrenberg et al., 1988), stains not only the mitochondria but also the cytosol of inner-zone cells much more strongly than those of the outer-zone cells (Hirano et al., 2000). This implies that the plasma membrane of the inner-zone cells is somewhat hyperpolarized compared to that of outer-zone cells and is quite the opposite of what one would expect if the patterning were determined merely by inhibition of plasma membrane proton pumps in the inner-zone cells. In this light, it would be interesting to see whether the plasma membrane proton pump encoding gene *patB*, which is known to be highly expressed under acidic conditions (Coukell et al., 1997), is expressed in the inner-zone cells.

#### A reaction scheme

As we saw with weak acid/base and proton pump inhibition experiments, altering either pH or intracellular buffering capacity has a strong influence on the patterning. It is known that *Dictyostelium* development relies on catabolism of about 50% of its protein and RNA. As a result, a large amount of

TCA-cycle intermediates and related metabolites (Kelly et al., 1979) and ammonia (Schindler and Sussman, 1977) are released from the cells. Under 2-D culturing conditions, outward proton pumping by the plasma membrane H-ATPase may be partially blocked by the low oxygen levels. It is known that under such conditions, where ionic regulation is suppressed, cellular pH depends more on the acid-base balance of metabolites accumulated in the extracellular and intracellular space (Pörtner, 1993). Thus secreted organic acids and ammonia could play important roles in the rapid patterning by causing pHi changes.

Another explanation for the patterning is that cells respond to a threshold level of oxygen (Bonner et al., 1998). We have calculated the oxygen level in the 2-D cell mass based on the reported oxygen consumption rate of *Dictyostelium* cells (Sternfeld and David, 1981; Krill and Town, 1988) and find it difficult to explain the known oxygen dependency of outer-zone size or other inherently nonlinear patterning properties (Bonner et al., 1998; Sawai et al., 2000).

Two earlier studies suggest a strong correlation between oxygen and ammonia production. Bonner et al. (1990) reported a rapid bleaching of Neutral-Red staining of the posterior region of a young slug which occurs within 10 min when it is submerged under mineral oil. This could be explained by stabilization of an ammonia gradient triggered by low oxygen. Sternfeld (1988) observed that when a slug is transferred to 100% O<sub>2</sub> environment, Neutral-Red staining of the anterior region is also bleached due to higher ammonia production by prestalk cells. Although the pattern of bleaching is different, these findings suggest that altering the oxygen concentration has a significant influence on ammonia production and hence acid-base balance of the *Dictyostelium* cells.

We propose that there are two major diffusive players in the patterning, (1) Y, a fast-diffusing ammonia or other weak base that raises the pHi and/or the pH of other intracellular compartments, and (2) X, a weak acid or its precursor produced as a result of protein degradation. A possible scheme is shown in Fig. 6A, in which Y acts as a substrate for further generation of X. This is the so-called substrate-depletion type reaction, which is well known to generate self-organized patterns when coupled with diffusion (Nicolis and Prigogine, 1977; Meinhardt, 1982; Harrison, 1993). Since X acts to decrease pHi, and Y is a molecule with the opposite effect, it is easy to understand why such a sudden drop in pHi was observed at the border between the outer and the inner zone (Fig. 6B). In the scheme, oxygen has a role of giving polarity to the patterning. Higher oxygen implies more production of ammonia (Y), which means that the peak of Y is always at the outer zone edge.

The scheme resembles the weak-acid and weak-base model (MacWilliams and Bonner, 1979; Inouye, 1990). However, the current model predicts X and Y to have peaks at different locations, which are not achievable by those previous models based on activator-inhibitor type equations. The main difference is that ammonia is consumed for the production of X in our model. Such a positive role for ammonia has been

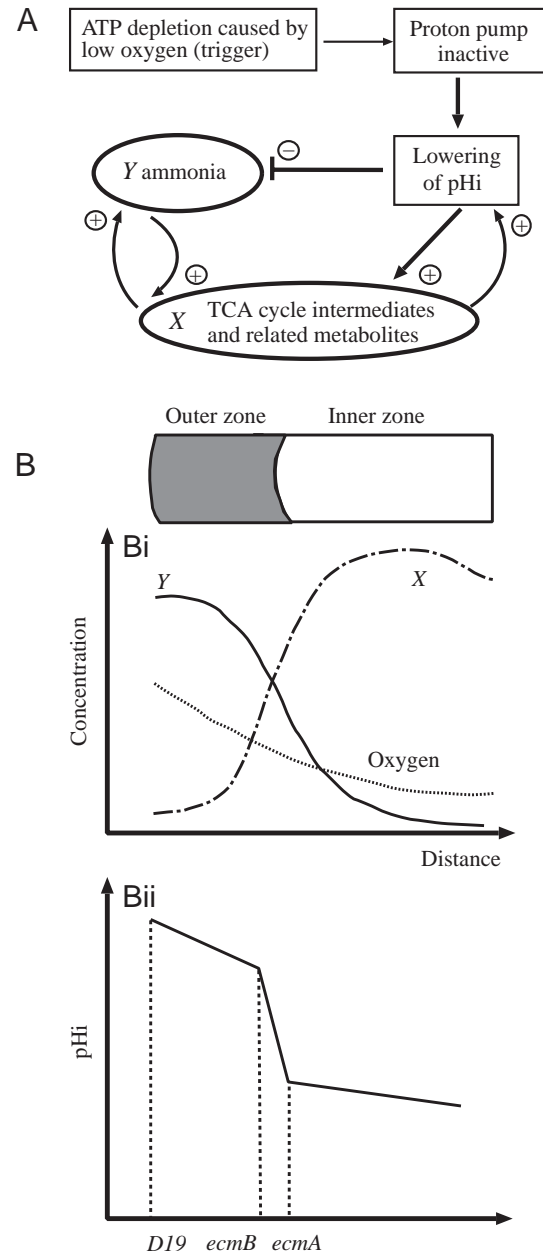


Fig. 6. A diagram of the proposed reaction scheme. (A) Low oxygen acts as a trigger to lower pHi, which enhances protein degradation. As a result, weak acids and other related metabolites (X) increase, which further lowers pHi. At the same time, ammonia (Y) is produced as the final end product. Ammonia, being a small neutral molecule, could permeate the cell membrane easily compared to weak acids, resulting in a large difference in their diffusion coefficient, which is a required condition for the Turing instability (Nicolis and Prigogine, 1977). When the pH is low, ammonia levels will decrease by protonation. Y is consumed in an oxygen-dependent fashion for the production of X by transamination, thus realizing a substrate-depletion type reaction (Meinhardt, 1982). (B) Reaction and diffusion of X and Y creates a stationary gradient with each peak positioned off-phase from each other (Bi). Gradients of X and Y influence pHi and, furthermore, cell differentiation (Bii). The positions of *D19*, *ecmA* and *ecmB* gene expression are also indicated (see text for details).

proposed by Cotter et al. (1992) as a source-sink model to explain the ammonia gradient within a slug. Given the role of ammonia as a substrate, it is natural that a higher initial content of ammonia hastened the patterning. Similarly, differentiating cells show much faster patterning compared to freshly starved cells (S. Sawai, unpublished observation). This may also be due to the higher content of ammonia or higher activity of ammonia-regulating enzymes such as AMP-deaminase (Jahngen and Rossomando, 1986) and NAD-dependent glutamate dehydrogenase (Pamula and Wheldrake, 1992) in the cells at the later stages of development.

#### Cell differentiation

The pH gradient presented in this paper could partially explain the zonal differentiation pattern reported earlier (Hirano et al., 2000). In the 2-D cultures, cells at the outermost region of the outer zone, where the pH is the highest, show prespore *D19* gene expression, followed by prestalk *ecmB* and then *ecmA* expressed just near the border (Fig. 6Bii). It should be noted that our findings are quite the opposite to what Bonner and his colleagues had first postulated based on their Neutral-Red staining results and oxygen alone as a factor giving preference to differentiation. Conditions that decrease pH favor prestalk and stalk cell differentiation (Gross et al., 1983, 1988; Kubohara and Okamoto, 1994; Dominov and Town, 1986; Wang et al., 1990). It is also known that incubation with weak bases such as ammonia and methylamine favors prespore cell differentiation (Gross et al., 1983; Neave et al., 1983; Davies et al., 1993). The slope of the pH gradient does not seem to differ so much when the oxygen concentration is high, thus pH may not explain why we observed more *ecmA* expression in the inner zone when oxygen was higher (Hirano et al., 2000). Low pH may impose only a bias toward the prestalk pathway and a more precise mechanism mediated by cAMP, DIF and ammonia must be involved in cell-type proportion regulation, even under the present culturing conditions.

The present findings provide clues as to what may take place in a normal aggregate developing in 3-D when oxygen becomes scarce. Oxygen depletion is a common phenomenon in soil, especially when the pores become filled with water and gas diffusion becomes limited (Baumgartl et al., 1994; Cooper and van Gundy, 1971; Drew, 1992). Broad oxygen tolerance is reported in the soil nematode (van Voorhies and Ward, 2000), which shares a natural habitat with *Dictyostelium* (Kessin et al., 1996). Although *Dictyostelium* development takes place in three dimensions, it is possible that situations similar to the 2-D culture, i.e. conditions of limited oxygen, as suggested by Sandona et al. (1995), and space, are encountered by developing *Dictyostelium* cells in soil. At present, there are two different views as to how the early cell differentiation takes place in *Dictyostelium*; one is a position-dependent mechanism (Maeda, 1993; Early et al., 1995) and the other is a cell-autonomous mechanism (Kay et al., 1999; Thompson and Kay, 2000). The present findings and the model suggest, at least under confined conditions, that an oxygen gradient

within a cell aggregate is converted to an ammonia or pH gradient. As has been postulated in many hypoxia-tolerant organisms, the pH response may reflect *Dictyostelium*'s defense mechanism to cope with oxygen depletion. Since cytoplasmic acidification is reported to facilitate induction of prestalk gene expression by DIF-1 (Wang et al., 1990), it may be that *Dictyostelium* development is well adapted to hypoxia.

We thank Lionel F. Jaffe, Kei Inouye, Ismael Rafols, Edward C. Cox and John T. Bonner for discussions and comments.

#### References

- Azhar, M. and Nanjundiah, V. (1996). Spatial patterning of the distribution of  $\text{Ca}^{2+}$  assayed in fine glass capillaries. *J. Biosci.* **21**, 765–774.
- Baumgartl, H., Kritzler, K., Zimelka, W. and Zinkler, D. (1994). Local  $\text{PO}_2$  measurements in the environment of submerged soil microarthropods. *Acta Oecologica* **15**, 781–789.
- Bonner, J. T. (1947). Evidence for the formation of cell aggregates by chemotaxis in the development of the slime mold *Dictyostelium discoideum*. *J. Exp. Zool.* **106**, 1–26.
- Bonner, J. T., Feit, I. N., Selassie, A. K. and Suthers, H. B. (1990). Timing of the formation of the prestalk and prespore zones in *Dictyostelium discoideum*. *Dev. Genet.* **11**, 439–441.
- Bonner, J. T., Compton, K. B., Cox, E. C., Fey, P. and Gregg, K. Y. (1995). Development in one dimension: the rapid differentiation of *Dictyostelium discoideum* in glass capillaries. *Proc. Natl. Acad. Sci. USA* **92**, 8249–8253.
- Bonner, J. T., Segel, L. and Cox, E. C. (1998). Oxygen and differentiation in *Dictyostelium discoideum*. *J. Biosci.* **23**, 177–184.
- Cooper, A. F. and van Gundy, S. D. (1971). Senescence, quiescence and crypobiosis. In *Plant Parasitic Nematodes*, vol. 2 (ed. B. M. Zuckerman, W. F. Mai and R. A. Rhode), pp. 297–318. New York: Academic Press.
- Cotter, D. A., Sands, T. W., Viridy, K. J., North, M. J., Klein, G. and Satre, M. (1992). Patterning of development in *Dictyostelium discoideum*: factors regulating growth, differentiation, spore dormancy, and germination. *Biochem. Cell Biol.* **70**, 892–919.
- Coukell, M. B., Moniakos, J. and Cameron, A. M. (1997). The *patB* gene of *Dictyostelium discoideum* encodes a P-type H-ATPase isoform essential for growth and development under acidic conditions. *Microbiol.* **143**, 3877–3888.
- Davies, L., Satre, M., Martin, J. and Gross, J. (1993). The target of ammonia action in *Dictyostelium*. *Cell* **75**, 321–327.
- Dominov, J. A. and Town, C. D. (1986). Regulation of stalk and spore antigen expression in monolayer cultures of *Dictyostelium discoideum* by pH. *J. Embryol. exp. Morph.* **96**, 131–150.
- Drew, M. C. (1992). Soil aeration and plant root metabolism. *Soil Sci.* **154**, 259–268.
- Early, A., Abe, T. and Williams, J. (1995). Evidence for positional differentiation of prestalk cells and for a morphogenetic gradient in *Dictyostelium*. *Cell* **83**, 91–99.
- Ehrenberg, B., Valerie, M., Wei, M.-D., Wuskell, J. P. and Loew, L. M. (1988). Membrane potential can be determined in individual cells from the nematode distribution of cationic dyes. *Biophys. J.* **53**, 785–794.
- Gross, J. D., Bradbury, J., Kay, R. R. and Peacey, M. J. (1983). Intracellular pH and the control of cell differentiation in *Dictyostelium discoideum*. *Nature* **303**, 244–245.
- Gross, J. D., Peacey, M. J. and Pogge von Strandmann, R. (1988). Plasma membrane proton pump inhibition and stalk cell differentiation in *Dictyostelium discoideum*. *Differentiation* **38**, 91–98.
- Hara, K. and Konijn, T. M. (1976). Effect of temperature on morphogenetic oscillations of *Dictyostelium discoideum*. *Nature* **260**, 705.
- Harrison, L. G., Snell, J., Verdi, R., Vogt, D. E., Zeiss, G. D. and Green, B. R. (1981). Hair morphogenesis in *Acetabularia mediterranea*: temperature-dependent spacing and models of morphogen waves. *Protoplasma* **106**, 211–221.
- Harrison, L. G. (1993). *Kinetic Theory of Living Patterns*. New York: Cambridge University Press.
- Haugland, R. P. (1996). Probes useful at near-neutral pH. In *Handbook of*

- Fluorescent Probes and Research Chemicals*, pp. 552–561. Eugene: Molecular Probes.
- Hirano, T., Sawai, S., Sawada, Y. and Maeda, Y. (2000). Rapid patterning in 2-D cultures of *Dictyostelium* cells and its relationship to zonal differentiation. *Dev. Growth Differ.* **42**, 551–560.
- Inouye, K. (1988). Differences in cytosolic pH and the sensitivity to acid load between prestalk cells and prespore cells of *Dictyostelium*. *J. Cell Sci.* **91**, 109–115.
- Inouye, K. (1989). Regulation of cytoplasmic pH in the differentiating cell types of the cellular slime mould *Dictyostelium discoideum*. *Biochim. Biophys. Acta* **1012**, 64–68.
- Inouye, K. (1990). Control mechanism of stalk formation in the cellular slime mould *Dictyostelium discoideum*. *Forma* **5**, 119–134.
- Jahngen, E. G. E. and Rossomando, E. F. (1986). AMP deaminase in *Dictyostelium discoideum*: increase in activity following nutrient deprivation induced by starvation or hadacidin. *Mol. Cell Biochem.* **71**, 71–78.
- Jungbluth, A., von Arnim, V., Biegelmann, E., Humbel, B., Schweiger, A. and Gerisch, G. (1994). Strong increase in the tyrosine phosphorylation of actin upon inhibition of oxidative phosphorylation: correlation with reversible rearrangements in the actin skeleton of *Dictyostelium* cells. *J. Cell Sci.* **107**, 117–125.
- Kay, R., Flatman, P. and Thompson, C. R. L. (1999). DIF signalling and cell fate. *Semin. Cell Dev. Biol.* **10**, 577–585.
- Kelly, P. J., Kelleher, J. K. and Wright, B. E. (1979). The tricarboxylic acid cycle in *Dictyostelium discoideum*. *Biochem. J.* **184**, 581–588.
- Kessin, R. H., Gundersen, G. G., Zaydfudim, V., Grimson, M. and Blanton, R. L. (1996). How cellular slime molds evade nematodes. *Proc. Natl. Acad. Sci. USA* **93**, 4857–4861.
- Krill, D. C. and Town, C. D. (1988). Arachidonate-dependent oxygen consumption in *Dictyostelium discoideum*. *J. Gen. Microbiol.* **134**, 2123–2179.
- Kubohara, Y. and Okamoto, K. (1994). Cytoplasmic  $\text{Ca}^{2+}$  and  $\text{H}^{+}$  concentrations determine cell fate in *Dictyostelium discoideum*. *FASEB J.* **8**, 869–874.
- MacWilliams, H. K. and Bonner, J. T. (1979). The prestalk-prespore pattern in cellular slime molds. *Differentiation* **14**, 1–22.
- Maeda, Y. (1993). Pattern-formation in a cell-cycle dependent manner during the development of *Dictyostelium discoideum*. *Dev. Growth Differ.* **35**, 609–616.
- Meinhardt, H. (1982). *Models of Biological Pattern Formation*, pp. 34–36. London: Academic Press.
- Neave, N., Sobolewski, A. and Weeks, G. (1983). The effect of ammonia on stalk cell formation in submerged monolayers of *Dictyostelium discoideum*. *Cell Differ.* **13**, 301–307.
- Newman, S. A. and Comper, W. D. (1990). ‘Generic’ physical mechanisms of morphogenesis and pattern formation. *Development* **110**, 1–18.
- Nicolis, G. and Prigogine, I. (1977). *Self-Organization in Nonequilibrium Systems*, pp. 90–159. New York: Wiley-Interscience.
- Pamula, F. and Wheldrake, J. F. (1992). The effect of AMP on the NAD-dependent glutamate dehydrogenase during activation and morphogenesis in the cellular slime moulds. *J. Gen. Microbiol.* **138**, 1935–1940.
- Pogge-von Strandmann, R., Kay, R. R. and Dufour, J.-P. (1984). An electrogenic proton pump in plasma membranes from the cellular slime mould *Dictyostelium discoideum*. *FEBS Lett.* **175**, 422–428.
- Pörtner, H.-O. (1993). Multi-compartmental analyses of acid–base and metabolic homeostasis during anaerobiosis: invertebrate and lower vertebrate examples. In *Surviving Hypoxia* (ed. P. W. Hochachka, P. L. Lutz, T. Sick, M. Rosenthal and G. van den Thillart), pp. 140–154. Boca Raton: CRC Press.
- Sandona, D., Gastaldello, S., Rizzuto, R. and Bisson, R. (1995). Expression of cytochrome c oxidase during growth and development of *Dictyostelium*. *J. Biol. Chem.* **270**, 5587–5593.
- Sawada, Y., Maeda, Y., Takeuchi, I., Williams, J. and Maeda, Y. (1998). Rapid patterning of *Dictyostelium discoideum* cells under confined geometry and its relation to differentiation. *Dev. Growth Differ.* **40**, 113–120.
- Sawai, S., Maeda, Y. and Sawada, Y. (2000). Spontaneous symmetry breaking Turing-type pattern formation in a confined *Dictyostelium* cell mass. *Phys. Rev. Lett.* **85**, 2212–2215.
- Schindler, J. and Sussman, M. (1977). Ammonia determines the choice of morphogenetic pathways in *Dictyostelium discoideum*. *J. Mol. Biol.* **116**, 161–169.
- Singleton, C. K., Zinda, M. J., Mykytko, B. and Yang, P. (1998). The histidine kinase *dhkC* regulates the choice between migrating slugs and terminal differentiation in *Dictyostelium discoideum*. *Dev. Biol.* **203**, 345–357.
- Sternfeld, J. (1988). Proportion regulation in *Dictyostelium* is altered by oxygen. *Differentiation* **37**, 137–179.
- Sternfeld, J. and David, C. N. (1981). Oxygen gradient causes pattern orientation in *Dictyostelium* cell clumps. *J. Cell Sci.* **50**, 9–17.
- Stoekelhuber, M., Noegel, A. A., Eckerskorn, C., Kohler, J., Rieger, D. and Schleicher, M. (1996). Structure/function studies on the pH-dependent actin-binding protein hisactophilin in *Dictyostelium* mutants. *J. Cell Sci.* **109**, 1825–1835.
- Thompson, C. R. L. and Kay, R. (2000). Cell-fate choice in *Dictyostelium*: intrinsic biases modulate sensitivity to DIF signaling. *Dev. Biol.* **227**, 56–64.
- van Duijn, B. and Inouye, K. (1991). Regulation of movement speed by intracellular pH during *Dictyostelium discoideum* chemotaxis. *Proc. Natl. Acad. Sci. USA* **88**, 4951–4955.
- van Duijn, B. and Vogelzang, S. A. (1989). The membrane potential of the cellular slime mold *Dictyostelium discoideum* is mainly generated by an electrogenic proton pump. *Biochim. Biophys. Acta* **983**, 186–192.
- van Duijn, B., Vogelzang, S. A., Ypey, D. L., van der Molen, L. G. and van Haastert, P. J. M. (1990). Normal chemotaxis in *Dictyostelium discoideum* cells with a depolarized plasma membrane potential. *J. Cell Sci.* **95**, 177–183.
- van Haastert, P. J. M., de Vries, M. J., Penning, L. C., Roovers, E., van der Kaay, J., Erneux, C. and van Lookeren Campagne, M. M. (1989). Chemoattractant and guanosine 5′-[γ-thio]triphosphate induce the accumulation of inositol 1,4,5-trisphosphate in *Dictyostelium* cells that are labelled with [ $^3\text{H}$ ]inositol by electroporation. *Biochem. J.* **258**, 577–586.
- van Voorhies, W. and Ward, S. (2000). Broad oxygen tolerance in the nematode *Caenorhabditis elegans*. *J. Exp. Biol.* **203**, 2467–2478.
- Wang, M., Roelfsema, J. H., Williams, J. G. and Schaap, P. (1990). Cytoplasmic acidification facilitates but does not mediate DIF-induced prestalk gene expression in *Dictyostelium discoideum*. *Dev. Biol.* **140**, 182–188.
- Watts, D. J. and Ashworth, J. M. (1970). Growth of myxameobae of the cellular slime mould *Dictyostelium discoideum* in axenic culture. *Biochem. J.* **119**, 171–174.
- Wurster, B. (1976). Temperature dependence of biochemical oscillations in cell suspensions of *Dictyostelium discoideum*. *Nature* **260**, 703–704.
- Yumura, S., Matsuzaki, R. and Kitanishi-Yumura, T. (1995). Introduction of macromolecules into living *Dictyostelium* cells by electroporation. *Cell Struct. Func.* **20**, 185–190.